Engineering and Technology Journal
Journal homepage: https://etj.uotechnology.edu.iq

Manufacturing of Sustainable Ultra-High-Performance Concrete Using Response Surface Methods

Abbas J. Mohammed[a,b]*, **Maan S. Hassan**[a], **Hussein Al-Quraishi**[a]

[a] Civil Engineering Dept., University of Technology-Iraq, Alsina'a street, 10066 Baghdad, Iraq.
[b] Civil Techniques Dept., Nasiriyah Technical Institute, Southern Technical University, Baghdad Street, Nasiriyah 64001, Iraq.
*Corresponding author Email: bce.20.09@grad.uotechnology.edu.iq

HIGHLIGHTS

- Quartz powder can be removed from ultra-high-performance concrete (UHPC) mixtures
- The inclusion of limestone powder in UHPC mixtures substantially improves compressive strength
- A 48hr-90°C curing regime is optimal for achieving the highest compressive strength

ARTICLE INFO

Handling editor: Mohammed A. Al-Neami

Keywords:
Ultra High-Performance Concrete (UHPC)
Optimisation
Response Surface Methodology (RSM)
Limestone Powder
Quartz Powder

ABSTRACT

Quartz powder is used in ultra-high-performance concrete to improve granular packing, but repeated inhalation during manufacture can cause health issues. The mechanical properties of UHPC are influenced by the post-setting curing method. A hypothesis suggests limestone powder could be a viable filler to mitigate these issues under three different curing regimes, replacing quartz powder of similar size. The study assessed 18 mixtures with different w/b ratios for flow characteristics and compressive strength after 7 and 28 days of curing under various conditions. Limestone powder positively impacted compressive strength and had fresh properties. A two-factor interaction model accurately correlated variables and responses. Numerical optimization was performed to find the optimal mixture with proper flow and the highest compressive strength. The use of 150 kg/m^3 of locally sourced limestone powder in the mixture with a w/b ratio equal to 0.198 and a 48hr-90°C curing regime can be considered the optimal amount to secure the greatest modeling compressive strength (169.10 MPa at 7 days and 181.71 MPa at 28 days), fulfilling the limit values of spread flow (220 mm) with the increasing percentage ratio of 67% and 49% at 7-days and 28-days ages under 90°C heat curing when the w/b equals 0.198.

1. Introduction

UHPC is a new cementitious composite invented in France in the early 1990s that exceeds standard concrete in terms of mechanical strength, energy absorption capacity, and durability [1]. By definition, the features of three unique types of specialty concrete mixes may be found in UHPC mix designs. High-performance concrete (HPC) offers improved strength (more than 150 MPa) and long-term performance; fiber-reinforced concrete (FRC) has greater ductility and post-cracking strength; and self-consolidating concrete (SCC) may flow and pass [2]. Figure 1 displays the self-consolidating ultra-high-performance fiber-reinforced concrete supplied to the construction sector due to incorporating the aforementioned concrete properties.UHPC is currently utilized in building footbridges, bridge joints between precast deck panels, special prestressed and precast concrete elements, long-span objects and skyscrapers, marine platforms, concrete repair, urban furniture, precast walls, and industrial floors. Other uses include blast protection elements, high-ductility designs, repair and strengthening overlays on damaged pavements, and various architectural uses [3-5].

The good properties of UHPC stem from the extraordinary uniformity of its mixture and the replacement of coarse material with tiny particles of common crystalline silica types, such as silica sand (SS) and quartz powder (QP) [6]. Long-term exposure to fine crystalline silica through inhalation and the demolition process can cause silicosis, fibrosis of the lungs that causes shortness of breath, a chronic cough, and potentially fatal lung lesions. According to the International Agency for Research on Cancer, crystalline silica poses a similar cancer risk to people [7-10]. Moreover, QP is more dangerous to breathe in than fine silica sand because it can become aerosolized more easily [9]. When the composition principle of UHPC was originally disclosed in the 1990s, the filler effect of QP was not yet introduced [11].

http://doi.org/10.30684/etj.2023.143595.1598
Received 06 October 2023; Received in revised form 29 October 2023; Accepted 04 November 2023; Available online 30 December 2023
2412-0758/University of Technology-Iraq, Baghdad, Iraq

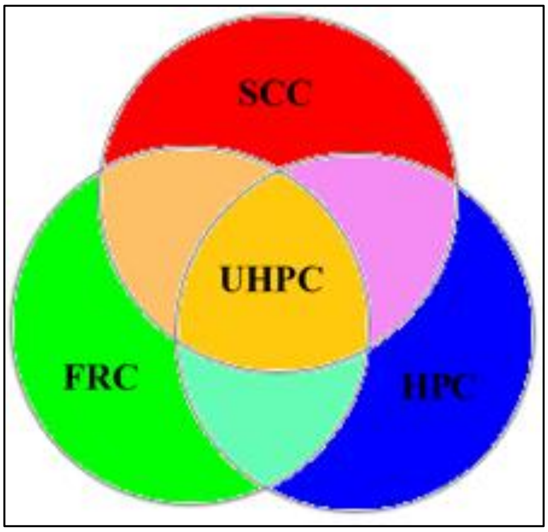

Figure 1: Different types of special concrete [2]

As an inert micro-aggregate, QP plays no active role in the operation of a UHPC. Its polymorphic mutation of β-quartz makes it highly pozzolanic when its particle size is less than 5 μm or when it is subjected to hydrothermal treatment at temperatures higher than 150°C. In addition, a high PH is needed [11-13]. Popular SCMs, such as fly ash and ground granulated blast furnace slag, may not be easily accessible in all areas. In addition, the UHPC materials should all be of the same high standard to guarantee the product's reliable performance [14].

Limestone powder is readily available in most parts of the world, is inexpensive, has very low embedded CO_2 emissions, and can be easily ground to a fine enough consistency to be used to make concrete [14-16]. Issues arise when limestone is used significantly to substitute cement in sub-zero climates. However, the combined use of limestone cement and pozzolans (silica fume, fly ash, etc.) increases the degree of hydration of both cement and silica fume in UHPC and inhibits the onset of the attack of sub-zero climates by decreasing permeability [15]. In addition to enhancing workability, a suitable proportion of limestone powder can have a good impact on the characteristics of concrete through filler nucleation and chemical reactions [16]. It is not yet known if the modification of the UHPC system's hydration process and mechanical properties upon substituting a part of the cement with LP is attributable to the special qualities of the LP or the mere physical effects of a mineral filler like QP [11].

Using LP instead of quartz powder in UHPC did not affect the material's strength or dimensional stability [11]. The curing process is essential for UHPC to develop its desired mechanical and durability qualities. Due to the low water contents, it is essential to increase the hydration reactions using the restricted amount of internal water and to take major precautions to prevent any water loss due to evaporation [17]. Prem et al., [18] concluded that 48 hours post-moulding-out is the optimal time for heat curing of UHPC. Most UHPC post-setting curing regimens retain concrete at 90°C with 90% humidity [19]. Heat curing transforms calcium hydroxide (CH) gel into calcium silicate hydrate (C-S-H) gel with increased strength during the hydration process [20]. The rate of hydration increases with increasing temperature; therefore, the thermal water cure has a greater impact on younger ages. To better shape hydrated structures, a thermal curing regime is preferable [21].

Conventional precast concrete requires a maximum temperature below 70°C to prevent delayed ettringite development [19]. Therefore, architectural UHPC precast elements are heat treated at 60°C for 72 hours with 95% relative humidity [22]. On-site circumstances may not be as beneficial as at precast UHPC operations. Accordingly, various studies examined conventional curing methods with some material circumstances at normal temperatures. The two curing regimes had similar compressive strengths at 91 days. However, particular material specifications and admixtures may cost more than heat curing for the cost-intensive UHPC [17]. This study aims to design and manufacture UHPC by avoiding using QP (replacing it with local limestone powder). The second objective is to track the type of heat curing regime on the strength. The design of the concrete mixtures was based on achieving great compressive strength and rheological properties with a minimum amount of QP. Response Surface Methodology (RSM) is used as a statistical design method to optimise UHPC dosage [23, 24].

2. Experimental Programmed

2.1 Materials

Portland cement with a specific gravity (g) of 3.15 and a mean particle diameter (d50) of 12.63 μm was utilized. Physical and chemical properties met ASTM C150/C150M (ASTM 2015a) [25]. Silica fume, with a 121% pozzolanic activity index, 2.20 g, and 0.16 μm d50, was used as a reactive powder per ASTM C1240-15 (ASTM 2015b) [26]. Local limestone powder (2.73 g, 7.11 μm d50) was employed as supplementary cementitious materials. XRD studies for LP were performed to determine the mineralogical compositions, as indicated in Figure 2.

The presence of calcite peaks indicates that calcium, primarily calcite, dominates the limestone.

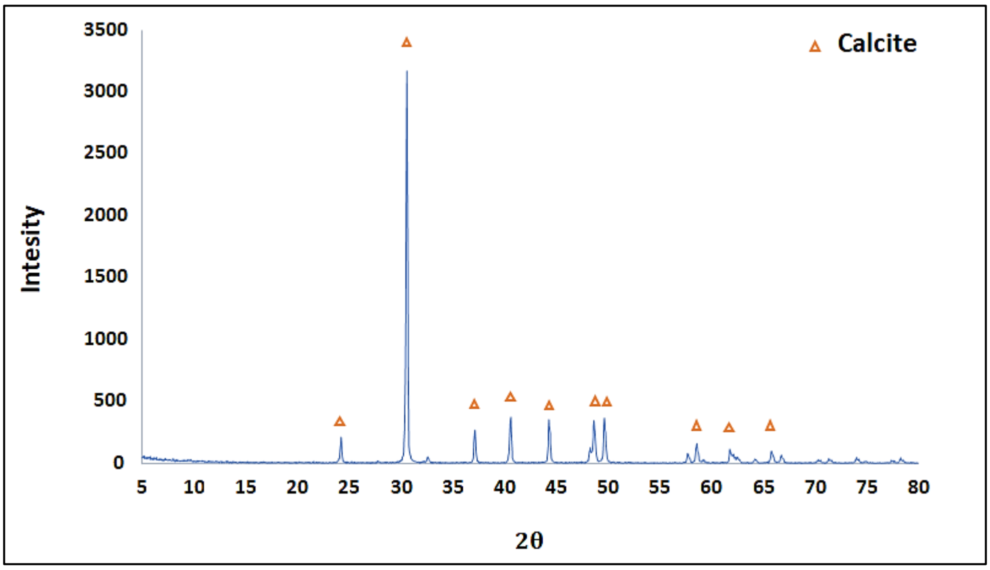

Figure 2: X-ray diffractogram of the local LP

2.2 Natural Aggregates, Steel Fiber, and Chemical Admixture

This investigation used fine quartz sand at 40% Sikadur 504 (80 µm to 0.2 mm) and 60% Sikadur 507 (0.3 to 0.85 mm). Blended fine sand had a 1500 kg/m^3 density and a specific gravity 2.7. Moreover, a quartz powder with an average particle size of 8 µm was used as a filler. Straight copper-coated micro-steel fibres were used. Aspect ratios were 65–94, and fiber lengths were 15–17 mm. Steel's ultimate tensile strength was 2991 MPa. Fibbers used 2% of the concrete volume. High-performance polycarboxylic polymer-based HRWR Hyperplast PC202 has a specific gravity of 1.07, a pH of 6, a solid content of 40%, and a chloride-free composition. The raw materials were subjected to an X-ray fluorescence (XRF) test to identify their chemical compositions, as shown in Table 1.

Also, Figure 3 shows Portland cement, silica fume, quartz sand, silica sand, and limestone powder particle size distributions.

Table 1: Chemical composition of cement, silica fume, limestone powder, and sand

Oxide	Cem	Sf	Lp	Sikadur 504	Sikadur 507
LOI	1.6	1.75	35.69	-	-
Na_2O	1.88	0.68	0.79	0.01	0.02
MgO	1.92	1.11	0.27	-	-
Al_2O_3	2.33	0.26	0.25	1.16	0.35
SiO_2	17.70	82.43	2.82	63.59	66.24
P_2O_5	0.07	0.05	-	0.02	0.03
SO_3	3.77	1.86	0.05	0.23	0.08
Cl	0.04	0.22	0.01	0.04	0.03
K_2O	1.02	3.83	0.02	0.01	-
CaO	68.38	1.82	59.88	0.71	0.19
TiO_2	0.25	0.01	0.01	0.63	0.02
Cr_2O_3	0.01	-	-	-	-
MnO	0.23	0.09	-	-	0.01
Fe_2O_3	5.10	1.02	0.17	0.16	0.06
ZnO	0.01	0.06	-	-	-
SrO	0.08	0.01	0.01	-	-
ZrO_2	0.01	-	-	0.53	0.01
Ba	0.10	-	-	-	-
Ta_2O_5	0.01	0.01	0.01	0.01	0.01
PbO	0.02	0.03	-	-	-

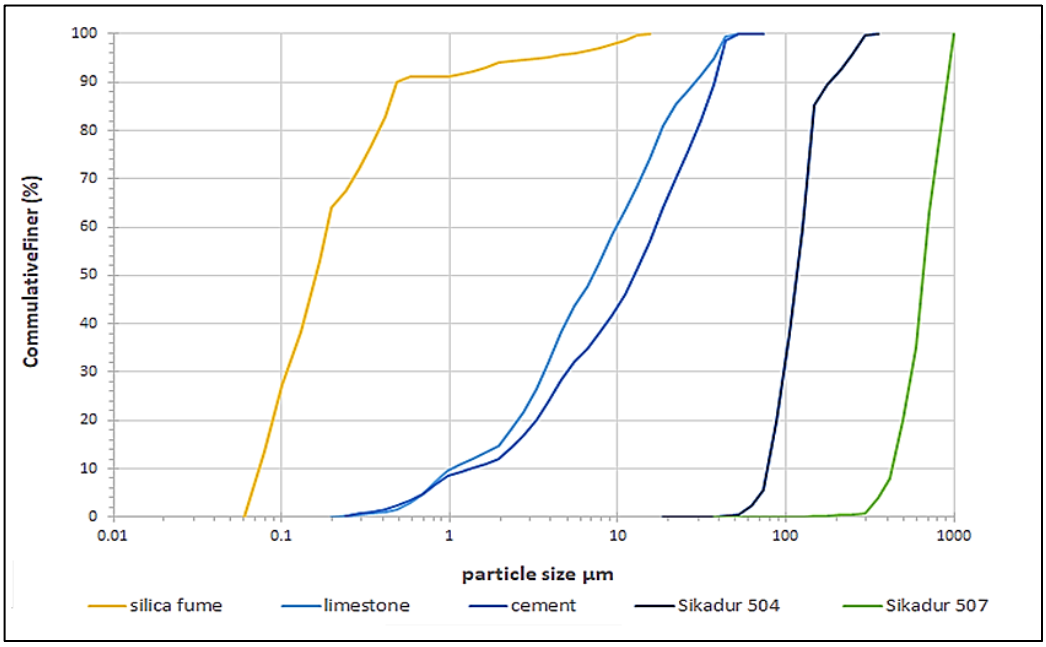

Figure 3: Raw material particle size distributions

2.3 Mix Proportions Selection and Curing Conditions

According to Kassel University formula M3Q_210, 18 UHPC mixes were planned and produced with different w/b, separated into three series. The first series 6 mixes eliminated QP and LP from the mixture. The second series 6 mixes were created by adding LP to the mixture to investigate the effect of LP. The third series was created by replacing LP with QP. The impact of curing on the characteristics of UHPC was studied using three different curing methods. After demolding, Cube specimens were stored under one of the following conditions: i. 48 hours of heat curing at 90°C, then normal curing at 20°C; ii. 72 hours of heat curing at 60°C, then normal at 20°C; or iii. continuous normal curing at 20°C. Table 2 presents the composition ratios of each constituent per cubic meter of freshly mixed concrete.

Table 2: Mix proportions as kg/m^3 of concrete

MIX	Cement	Silica fume	Limestone powder	Quartz powder	Total sand	Water	HRWR	Fibre	Curing degree
E1	852	200	0	0	990	177	42.08	154.88	24
E2	852	200	0	0	990	177	42.08	154.88	60
E3	852	200	0	0	990	177	42.08	154.88	90
E4	850	185	0	0	990	185	41.40	154.86	24
E5	850	185	0	0	990	185	41.40	154.86	60
E6	850	185	0	0	990	185	41.40	154.86	90
L1	772	145	150	0	990	177	36.68	154.88	24
L2	772	145	150	0	990	177	36.68	154.88	60
L3	772	145	150	0	990	177	36.68	154.88	90
L4	750	145	150	0	990	185	35.08	154.91	24
L5	750	145	150	0	990	185	35.08	154.91	60
L6	750	145	150	0	990	185	35.08	154.91	90
Q1	773	145	0	160	990	177	31.21	154.87	24
Q2	772	145	0	160	990	177	31.41	154.85	60
Q3	772	145	0	160	990	177	31.41	154.85	90
Q4	767	145	0	160	990	185	24.92	154.89	24
Q5	767	145	0	160	990	185	24.92	154.89	60
Q6	767	145	0	160	990	185	24.92	154.89	90

2.4 Mixing and Items of Investigation

A 10-litre mortar mixer made concrete after the dose design. After mixing, the flow-testing mold was full in 5 minutes. Cast and vibrate 50-mm compressive-strength cubes. The cube molds were fully wrapped in polythene for 24 hours before curing at 20 ± 2°C. The static slump flow diameter was determined in accordance with ASTM C1437 (ASTM 2020a) after mixing [27]. The compressive strength was calculated by testing 50-mm cubes. The ASTM C109/C109M-11b specification (ASTM 2010a) standard [28] was adhered to while using 3000 kN compression testing equipment. Three samples were analyzed for each of the ages of 7 and 28 days.

3. Results and Discussion

3.1 Flow Test

Figure 4 shows the results of the flow test for 18 mixtures. It is clear that quartz has the greatest effect on the flow rate, as mixtures containing quartz had the highest flow rate using the least amount of plasticizer and water. The flow rate of the Q1, 2, and 3 mixtures is approximately 232 mm with a water-cement ratio of 0.182 and HRWR (% solid content) of 1.16. In addition, when the ratio of water to cement was increased to 0.187, and the ratio of HRWR was reduced to 0.93, a flow rate of approximately 229 mm was obtained, which is also high. This result is in agreement with Rashad [29],who discovered that the workability of mixtures containing QP (up to 30%) in a blended slag is roughly 3.5 times higher than combinations without QP. Moreover, Rashad & Ouda [30], found that adding 30% QP to alkali-activated fly ash (AAFA) pastes enhances workability by filling particle packing spaces, reducing water requirements, and improving mixing efficiency.

Other observations that can be observed from Figure 4 are that it is possible to obtain a flow rate for mixtures containing limestone powder that is close to the flow rate for mixtures that do not contain any mineral additive, with a lower content of plasticizer and water. In contrast, the flow rate for L1,2,3 was 191 mm with a water-cement ratio of 0.187 and an HRWR of 1.38%, compared to 187 mm for the mixtures E1,2,3. Additionally, the flow rate of mixtures L4,5,6 was 219 mm with a water-cement ratio of 0.197 and a plasticizer of 1.36%, compared to the mixtures E4,5,6 with a 215 mm rate flow, a 0.203 water-cement ratio, and a plasticizer of 1.6%. These findings are consistent with those of the literature [9], [16], and [31], which found that adding limestone powder to a UHPC system can increase its potential for workability [9]. Adding limestone powder to a UHPC system reduced the superplasticizer needed [16, 31]. Limestone powder can improve the fluidity of the UHPC system by acting as a mineral plasticizer. This is due to its limited nucleation and chemical effects, neutral surface with Ca^{2+} and CO_3^{2-} ions, and weaker adsorption ability than cement and micro-silica. This results in reduced adsorption of polycarboxylic ether-based (PCE) molecules and reduced superplasticizer saturation dosages, enhancing the workability of the system [16].

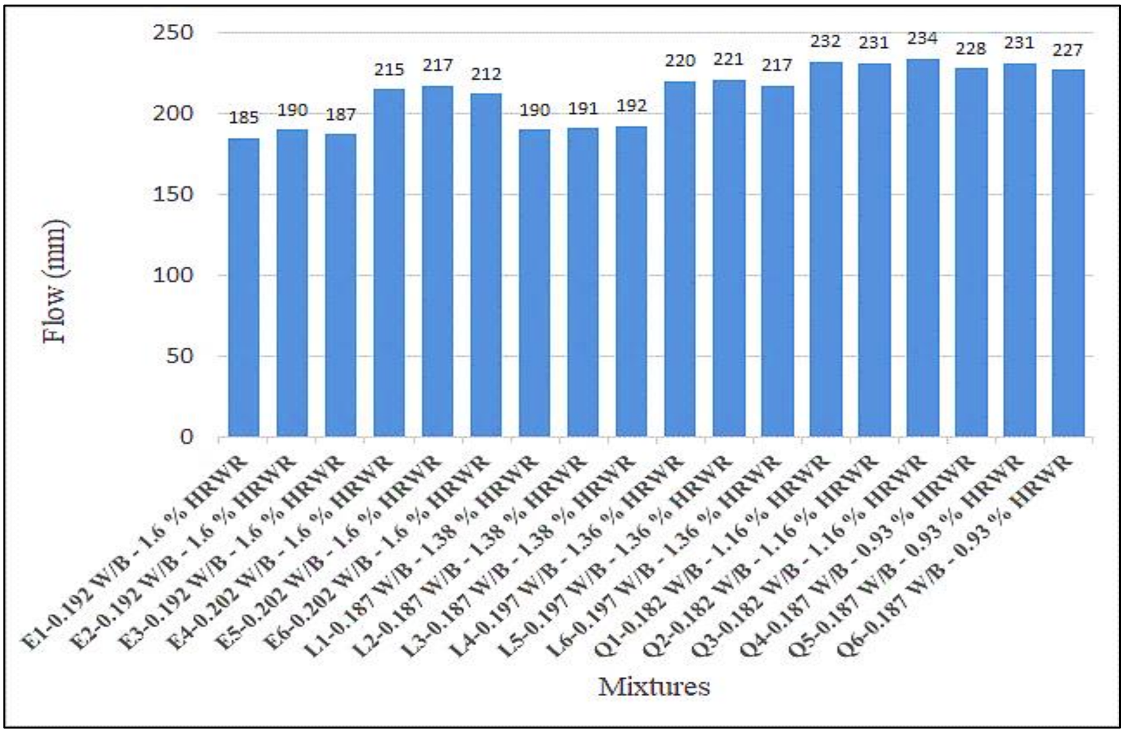

Figure 4: Flow test results

3.2 Seven Days of Compressive Strength

The 7-day compressive strength results are illustrated in Figure 5. It is clear to note the effect of adding local limestone powder on the compressive results of ultra-high-performance concrete mixes, as most of the mixtures containing limestone were higher than their counterparts of similar curing types. The compressive strengths of mixture L1 using normal curing at 24 °C were 133.8 MPa. At a curing level of 60 degrees, the concrete mixture L5 had the highest compressive strength at 147.8

MPa, followed by the mixture without any additive E2 at 147.4 MPa. When heat curing at 90°C was used, the limestone mixture produced high-performance concrete with a compressive strength exceeding 150 MPa. Whereby, the 7-day strength results for the L3 and L6 mixtures equal 156.7 and 178.8 MPa, respectively. According to M. A. Mosaberpanah et al., the temperature at which UHPC is curing significantly impacts its compressive strength when it is young [13]. On the other hand, the E6 mixture gave a result of 163.3 MPa but used a higher cement content and HRWR quantity. Huang et al., [14] indicated that the addition of limestone to UHPC improved the hydration degree of the cement from 39% in the traditional UHPC to 66%, and it helped ensure an even distribution of hydrates by serving as a nucleation and growth site for C-S-H on the outer surface. On the other hand, adding quartz powder to the UHPC decreased compressive strength; the best compressive result over a seven-day lifespan in the presence of quartz was 124.6 MPa for the Q3 mixture with a curing degree of 90°C. This may be because QP, as a microaggregate in UHPC design, does not exhibit significant pozzolanic activity when its particle size is greater than 5 mm or subjected to hydrothermal treatment less than 150°C [12].

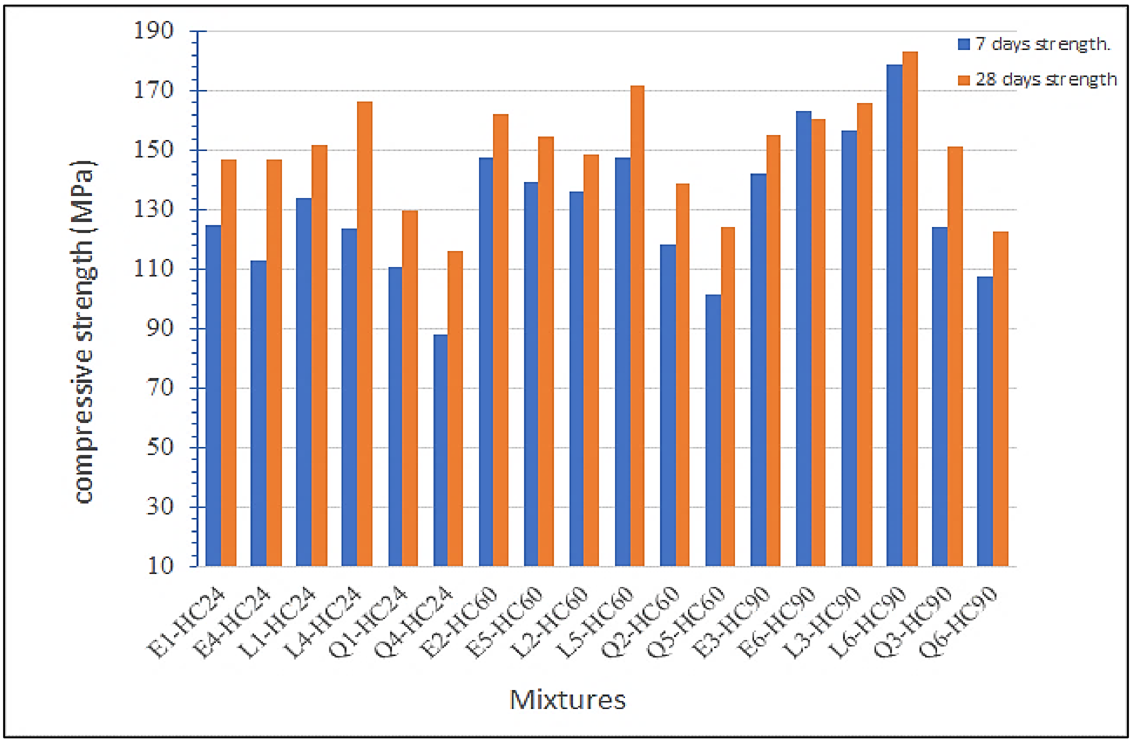

Figure 5: Compressive strength results

3.3 Twenty-Eight Days Compressive Strength

As shown in Figure 5, limestone powder had the greatest effect on compressive strength. All mixtures exceeded the minimum required for UHPC. In addition, it gave the highest results in all curing conditions. The compressive strength results for L4, 5, and 6 were 166.8, 172, and 183.4 MPa at a curing temperature of 24, 60, and 90 °C, respectively. For mixtures without mineral additives, no mixture was able to exceed the limit of 150 MPa when the curing temperature was 24 °C. When using heat curing at 60 and 90 °C, the mixtures exceeded the minimum limit, although they contained a high amount of cement and HRWR admixture.

In the team of mixtures containing quartz, the compressive strength was significantly affected by the water temperature used in the curing process, especially at the early ages. Whereas the compressive strength at 7 days ages increased by (7% and 12%) when the degree of heat curing changed to (60 °C and 90 °C) respectively. Moreover, when the w/b ratio increased, the compressive strength at 7 days age was clearly increased by (17% and 22%). This is due to hypothesizing that when subjected to high-temperature curing, silica fume and crushed quartz would exhibit elevated pozzolanic activity [32]. However, only one mixture (Q3) exceeded the minimum required for UHPC.

The strength result was 151.2 MPa using heat curing at 90 °C. This finding agrees with references [17, 21, 33], which found that the compressive strength of UHPC was significantly affected by the temperature of curing water due to the rate of hydration increasing with increasing temperature. Moreover, the thermal water cure has a greater impact on t early ages, and the formation of hydrated structures is improved by a thermal curing regime. In addition Prem et al., [18] observed that If the proper heat regime is not applied during curing, the silica fume and quartz powder in UHPC will only serve as filler materials, not as binders, rendering the UHPC useless. A solid skeleton is formed via the progressive production and rearrangement of hydration products, which is responsible for the development of strength, all of which occurs concurrently as a result of the chemical reaction of the binders .

3.4 Optimization

Design expert 13 program was used to model and optimize this study's variables and responses. Table 3 presents the model's ordering and experimental response values.

Table 3: Compositions and Experimental Response Values of Each Mixture

MIX	Parameter				Response		
	Limestone powder Kg/m^3	Quartz powder Kg/m^3	Heat curing degree °C	W/B ratio	7 days compressive strength (MPa)	28 days compressive strength (MPa)	Flow (mm)
E1	0	0	24	0.192	124.67	147.08	185
E2	0	0	60	0.192	147.37	162.15	190
E3	0	0	90	0.192	142.44	155.29	187
E4	0	0	24	0.203	112.93	147.00	215
E5	0	0	60	0.203	139.77	154.58	217
E6	0	0	90	0.203	163.29	160.34	212
L1	150	0	24	0.187	133.84	151.76	190
L2	150	0	60	0.187	136.15	148.91	191
L3	150	0	90	0.187	156.70	165.83	192
L4	150	0	24	0.197	123.92	166.76	220
L5	150	0	60	0.197	147.76	172.04	221
L6	150	0	90	0.197	178.82	183.41	217
Q1	0	160	24	0.182	110.80	129.49	232
Q2	0	160	60	0.182	118.54	138.98	231
Q3	0	160	90	0.182	124.58	151.16	234
Q4	0	160	24	0.186	88.06	116.25	228
Q5	0	160	60	0.186	101.78	124.40	231
Q6	0	160	90	0.186	107.36	122.80	227

3.4.1 Model verification

A two-factor interactions model (2FI) was derived for each response using Equation 1. And then computed using a sequential F-test. Regression analysis estimated parameters (K_1 to k_{10}), and the backward elimination method was used to remove non-significant terms.

$$\text{Response} = K1A+K2B+K3C+K4D+K5AB+K6AC+K7AD+K8BC+K9BD+K10CD \quad (1)$$

The final model predicts compressive strength at 7 days (R_7), 28 days (R_{28}), and spread flow (S). The model underwent ANOVA and a lack-of-fit test to determine its significance and sufficiency, with a P-value over 0.05 indicating an inconsequential mismatch between the variables. The ultimate models obtained to estimate the UHPC's compressive strength and flow are listed in Table 4.

Table 4: ANOVA for Reduced 2FI model

Model	R_7		R_{28}		S	
	Coeff.	**p-value**	**Coeff.**	**p-value**	**Coeff.**	**p-value**
Intercept	95.87	< 0.0001	120.95	< 0.0001	218.91	< 0.0001
A-LP	4.95	0.0344	10.30	< 0.0001	9.35	< 0.0001
B-QP	-46.85	0.0003	-43.55	< 0.0001	8.56	0.0137
C-Hc	21.28	< 0.0001	6.70	0.0005	-	-
D-w/b	-12.11	0.0070	-7.77	0.0199	4.75	0.0021
AB	-	-	-	-	-	-
AC	-	-	-	-	-	-
AD	-	-	5.32	0.0034	-	-
BC	-	-	-	-	-	-
BD	-14.06	0.0027	-12.66	0.0009	-9.79	< 0.0001
CD	5.53	0.0023	-	-	-	

Table 5 displays the F Statistic value and P-value for complete regression models. Additionally, it displays the projected coefficient of multiple determinations (Pre-R^2), the adjusted coefficient of multiple determinations (Adj-R^2), and adequate precision values (Adeq Precision).

Table 5: ANOVA and fit statistics values of the model

Responses	R^2	Adj-R^2	Pre-R^2	Adeq Precision	F-value	P-value
R_7	0.9519	0.9256	0.8924	20.1765	36.26	< 0.0001
R_{28}	0.9557	0.9316	0.8846	22.5291	39.57	< 0.0001
S	0.9891	0.9858	0.9794	40.7449	295.58	< 0.0001

The ANOVA's P-values indicated a negligible mismatch, with all P-values being less than 0.0001. The suitability of each suggested model was also verified using coefficients of multiple determination (R^2). whereas R^2 for the associations between variables R_7, R_{28} and S were 95.2%, 95.6 % and 98.9%. Also, The model excludes extraneous factors, with Adj-R^2 values close to R^2. The Predicted R² is in reasonable agreement with the Adjusted R², i.e., due to the difference being less than 0.2. also, Adeq Precision measures the signal-to-noise ratio. A ratio greater than 4 is desirable. This model can be used to navigate the design space from a high correlation coefficient and demonstrates the model's accuracy in predicting performance gains.

3.4.2 Model checking

In general, residuals are used to assess model adequacy. The residual plot pattern should be structureless for a good model. Each RSM's residuals sit near a straight line in the normal probability plot in Figures 6a, 7a, and 8a, indicating that errors are distributed normally and supporting the model's major terms. Figures 6b, 7b, and 8b compare expected and actual reaction levels. It helps identify values or groups that the model cannot predict. Any reaction abnormalities are shown in the figure.

Model equations and three-dimensional (3D) surfaces Figures 9, 10, and 11 show the interplaying effects of the study's independent variables on the responses. Where, (a) refers to that limestone powder amount in the mixture and the curing conditions fixed at high levels (150 Kg/m^3 and 90 °C, respectively), and (b) refers to that limestone powder amount in the mixture and the curing conditions fixed at low levels (0 Kg/m^3 and 24 °C, respectively). Based on Figures 9a, 9b, 10a, and 10b, the relationship between the studied independent variables and compressive strengths at both ages 7 and 28 days seemed to be non-linear. However, similar trends were observed between flow and independent variables (i.e., non-linear), as shown in Figures 11a and 11b, but with a higher degree of nonlinearity. Likewise, the interaction effects of these characteristics on the responses that were previously addressed were represented in these correlations.

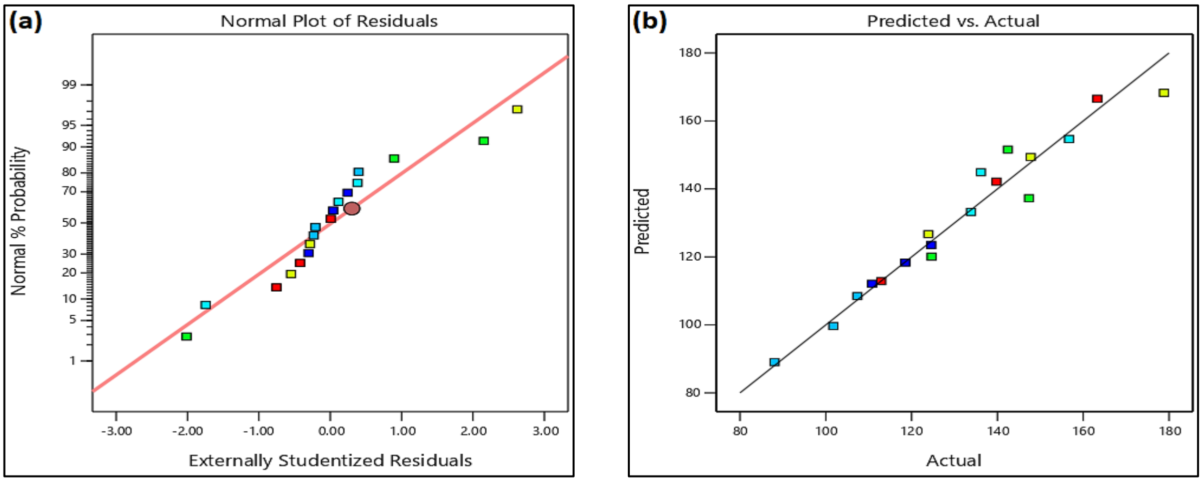

Figure 6: :(a) Normal plot of residuals; (b) Predicted versus actual values for R7

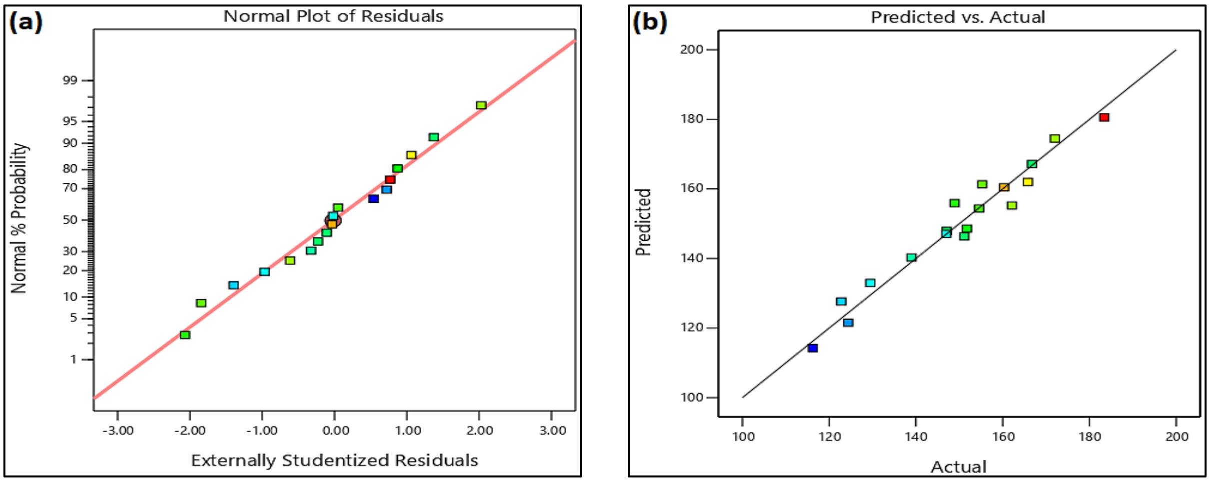

Figure 7: (a) Normal plot of residuals; (b) Predicted versus actual values for R28

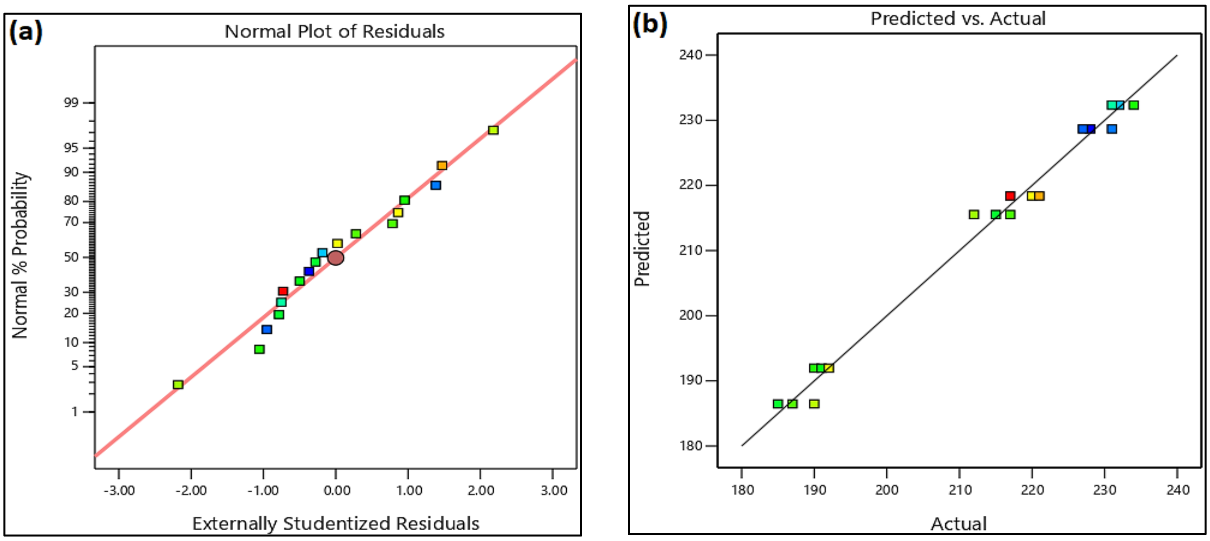

Figure 8: (a) Normal plot of residuals; (b) Predicted versus actual values for flow

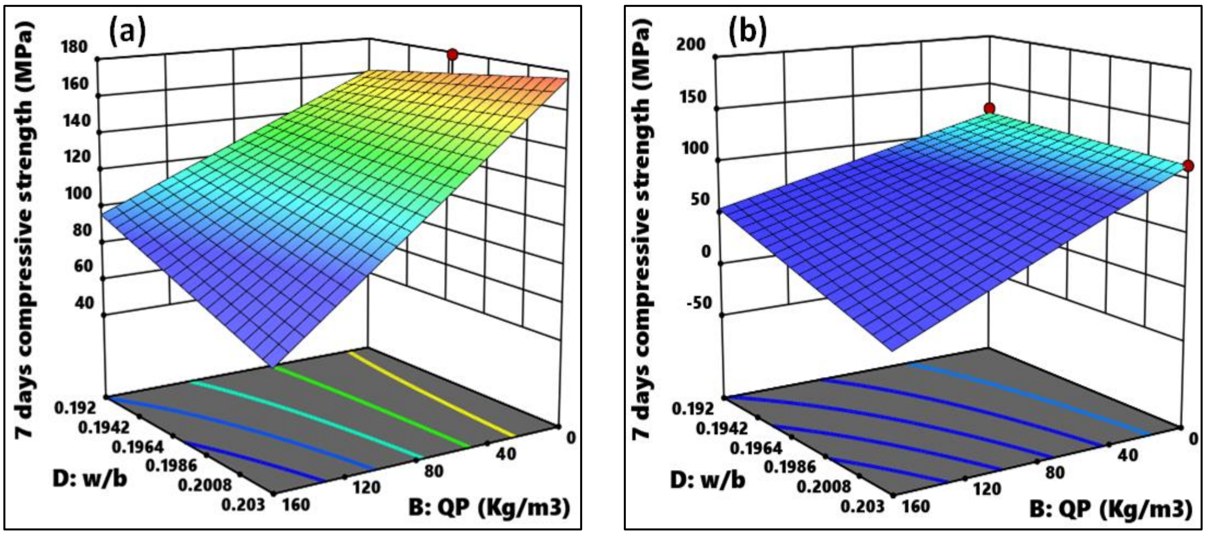

Figure 9: Response surface 3-D plots indicate the interaction effects of w/b and QP content on 7-day compressive strength. (a) Limestone powder and heat curing were fixed at high levels (150 Kg/m^3 and 90 °C, respectively); (b) Limestone powder and heat curing were fixed at low levels (0 Kg/m^3 and 24 °C, respectively).

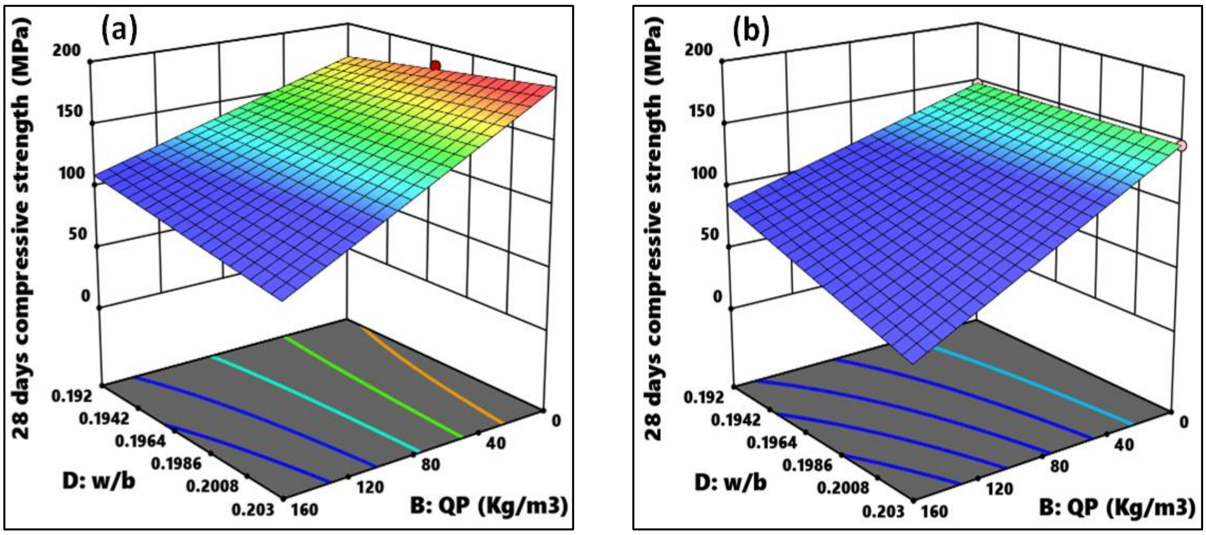

Figure 10: Response surface 3-D plots indicate the interaction effects of w/b and QP content on 28-day compressive strength. (a) Limestone powder and heat curing were fixed at a high levels (150 Kg/m^3 and 90 °C, respectively); (b) Limestone powder and heat curing were fixed at a low levels (0 Kg/m^3 and 24 °C, respectively).

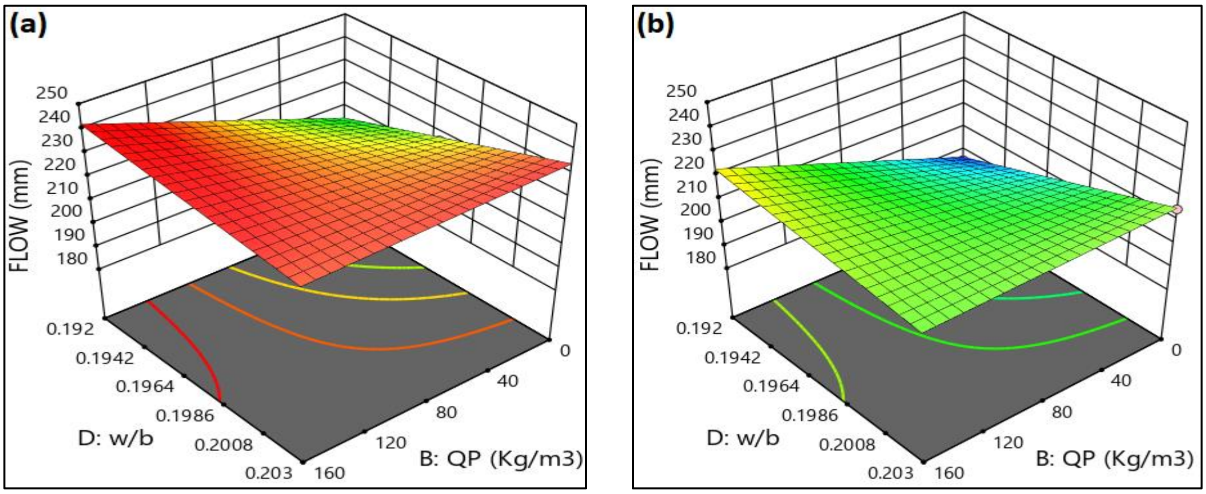

Figure 11: Response surface 3-D plots indicate the interaction effects of w/b and QP content on flow. (a) Limestone powder was fixed at a high level (150 Kg/m^3); (b) Limestone powder was fixed at a low level (0 Kg/m^3).

3.4.3 Optimum solutions output of model

The model can be optimized after validation and verification. Each response should be maximised, minimised, within a range to optimize. Additional requirements, like component weight and relevance, may be influenced by replies. The optimization output displays appropriate parameter values for optimal results based on requirements. This study used the proposed model to apply optimization criteria to maximize the 7 and 28-day compressive strength while seeking a flow within an acceptable range of 200 to 220 mm. At this stage, the LP was maximized, minimized QP content to reduce the adverse effects of QP, heat curing condition, and w/b ratio selected as in range. The optimization criteria and their conditions are listed in Table 6.The optimization output is listed in Table 7. Solutions were selected depending on the maximum desirability.

It should be noted that the QP can be eliminated from the UHPC mixture without any effects on the fresh and hard properties of UHPC by using heat curing at 90°C with the addition of LP.

Table 6: Optimization of Individual Responses for a UHPC Mixture with High Compressive Strength and Acceptable Fresh Properties

optimization criterion							
Parameters	**target**	**Lower**	**upper**	**Responses**	**target**	**Lower**	**upper**
LP (Kg/m^3)	maximize	0	150	R_7, MPa	maximize	150	180
QP (Kg/m^3)	minimize	0	150	R_{28}, MPa	maximize	150	185
Heat curing °C	In range	24	90	Flow, mm	In range	200	220
w/b ratio	In range	0.192	0.203				

Table 7: Output of optimization

Solution for optimization criterion				
Parameters	**Optimum**	**Responses**	**Optimum**	**Desirability**
LP (Kg/m^3)	150	R_7, MPa	169.10	0.874
QP (Kg/m^3)	0	R_{28}, MPa	181.71	
Heat curing conditions	90	Flow, mm	220	
w/b ratio	0.198			

4. Conclusion

This study examined the impact of key parameters on the rheology and compressive strength of UHPC. Using these parameters, a statistical model was created. The results of the experimental program and model analysis led to the following conclusions:

1) A statistical model was developed and proven to optimize LP and QP content, heat curing condition, and w/b ratio for optimal UHPC mixtures with optimal spread flow mix responses and greatest compressive strength.
2) The presence of QP in the UHPC mixture negatively affects the compressive strength at all ages, despite its positive effect on the flow. The compressive strength of mixtures with QP compared to mixtures without QP at 7 days of age was reduced by (11%, 20%, and 13%) under (24 °C, 60 °C, and 90 °C) heat curing, respectively. At 28 days of age, the compressive strength reduction becomes (12%, 14%, and 3%) under (24 °C, 60 °C, and 90 °C) heat curing, respectively. Moreover, the lowering of compressive strength was clearer when the w/b ratio increased. The percentages of lowering are (22%, 27%, 34%) and (21%, 20%, 23%) at 7 and 28 days ages under (24 °C, 60 °C, 90 °C) heat curing, respectively.

3) QP replacement by LP in UHPC mixtures leads to significantly enhanced compressive strength, with an associated adverse effect on flowability. The compressive strength increased by (21%, 15%, and 26%) and (17%, 7%, and 10%) at 7 and 28 days of age under (24 °C, 60 °C, and 90 °C) heat curing, respectively. This percentage changes to (41%, 45%, 67%) and (43%, 38%, and 49%) at 7 and 28 days of age under (24 °C, 60 °C, 90 °C) heat curing when the w/b ratio increases.
4) Heat-curing conditions have a significant impact on compressive strength at early ages.
5) Adding LP to the UHPC mixture reduced the UHPC cost and had an environmental impact due to reducing the cement content and the HRWR dose.

Author contribution

Conceptualization, M. Hassan; A. Mohammed and H. Al-Quraishi; methodology, A. Mohammed; software, A. Mohammed; validation, A. Mohammed and M. Hassan; formal analysis, A. Mohammed; investigation, A. Mohammed; resources, A. Mohammed; data curation, A. Mohammed; writing—original draft preparation, A. Mohammed; writing—review and editing, M. Hassan; visualization, A. Mohammed and M. Hassan; supervision, M. Hassan and H. Al-Quraishi; project administration, M. Hassan. All authors have read and agreed to the published version of the manuscript.

Funding

This research received no specific grant from any funding agency in the public, commercial, or not-for-profit sectors.

Data availability statement

Not applicable.

Conflicts of interest

The authors do not have a conflict of interest.

References

[1] M. H. Akeed et al., Ultra-high-performance fiber-reinforced concrete. Part I: Developments, principles, raw materials, Case Stud. Constr. Mater., 17 (2022) e01290. https://doi.org/10.1016/j.cscm.2022.e01290

[2] N. M. Azmee and N. Shafiq, Ultra-high performance concrete: From fundamental to applications, Case Stud. Constr. Mater., 9 (2018) e00197. https://doi.org/10.1016/j.cscm.2018.e00197

[3] C. Wu, J. Li, and Y. Su, Development of ultra-high performance concrete against blasts: from materials to structures. Woodhead Publishing, 2018.

[4] Ç. Yalçınkaya and O. Çopuroğlu, Hydration heat, strength and microstructure characteristics of UHPC containing blast furnace slag, J. Build. Eng., 34 (2021) 101915. https://doi.org/10.1016/j.jobe.2020.101915

[5] A. Arora, A. Almujaddidi, F. Kianmofrad, B. Mobasher, and N. Neithalath, Material design of economical ultra-high performance concrete (UHPC) and evaluation of their properties, Cem. Concr. Compos., 104 (2019) 103346. https://doi.org/10.1016/j.cemconcomp.2019.103346

[6] S. D. Salahaddin, J. H. Haido, and G. Wardeh, The behavior of UHPC containing recycled glass waste in place of cementitious materials: A comprehensive review, Case Stud. Constr. Mater., 17 (2022) e01494. https://doi.org/10.1016/j.cscm.2022.e01494

[7] J. D. Redondo-Mosquera, D. Sánchez-Angarita, M. Redondo-Pérez, J. C. Gómez-Espitia, and J. Abellan-Garcia, Development of high-volume recycled glass ultra-high-performance concrete with high C3A cement, Case Stud. Constr. Mater., 18 (2023) e01906. https://doi.org/10.1016/j.cscm.2023.e01906

[8] N. A. Soliman and A. Tagnit-Hamou, Using glass sand as an alternative for quartz sand in UHPC, Constr. Build. Mater., 145 (2017) 243-252. https://doi.org/10.1016/j.conbuildmat.2017.03.187

[9] J. F. Burroughs, J. Shannon, T. S. Rushing, K. Yi, Q. B. Gutierrez, and D. W. Harrelson, Potential of finely ground limestone powder to benefit ultra-high performance concrete mixtures, Constr. Build. Mater., 141 (2017) 335-342. https://doi.org/10.1016/j.conbuildmat.2017.02.073

[10] J. Abellán, J. Fernández, N. Torres, and A. Núñez, Statistical optimization of ultra-high-performance glass concrete, ACI Mater. J., 117 (2020) 243-254. https://doi.org/10.14359/51720292

[11] S.-H. Kang, Y. Jeong, K. H. Tan, and J. Moon, The use of limestone to replace physical filler of quartz powder in UHPFRC, Cem. Concr. Compos., 94 (2018) 238-247. https://doi.org/10.1016/j.cemconcomp.2018.09.013

[12] N. Soliman and A. Tagnit-Hamou, Development of ultra-high-performance concrete using glass powder–Towards ecofriendly concrete, Constr. Build. Mater., 125 (2016) 600-612. https://doi.org/10.1016/j.conbuildmat.2016.08.073

[13] M. A. Mosaberpanah and O. Eren, Effect of quartz powder, quartz sand and water curing regimes on mechanical properties of UHPC using response surface modelling, Adv. Concr. Constr., 5 (2017) 481-492. https://doi.org/10.12989/acc.2017.5.5.481

[14] W. Huang, H. Kazemi-Kamyab, W. Sun, and K. Scrivener, Effect of cement substitution by limestone on the hydration and microstructural development of ultra-high performance concrete (UHPC), Cem. Concr. Compos., 77 (2017) 86-101. https://doi.org/10.1016/j.cemconcomp.2016.12.009

[15] G. Hernández-Carrillo, A. Durán-Herrera, and A. Tagnit-Hamou, Optimization of Ultra-High-Performance Concrete Using Soft and Hard Inert Fillers (Limestone and Quartz), ACI Mater. J., 119 (2022) 275-288. https://doi.org/10.14359/51734222

[16] P. P. Li, H. Brouwers, W. Chen, and Q. Yu, Optimization and characterization of high-volume limestone powder in sustainable ultra-high performance concrete, Constr. Build. Mater., 242 (2020) 118112. https://doi.org/10.1016/j.conbuildmat.2020.118112

[17] K. K. Aswed, M. S. Hassan, and H. Al-Quraishi, Effects of Curing Temperature and Chemical Admixture Type on Fresh Properties and Compressive Strength of Ultra High-performance Concrete, Eng. Technol. J., 40 (2022) 1448-1454. http://doi.org/10.30684/etj.2022.132300.1103

[18] P. R. Prem, A. Ramachandra Murthy, and B. H. Bharatkumar, Influence of curing regime and steel fibres on the mechanical properties of UHPC, Mag. Concr. Res., 67 (2015) 988-1002. https://doi.org/10.1680/macr.14.00333

[19] S.-H. Kang, S.-G. Hong, and J. Moon, Shrinkage characteristics of heat-treated ultra-high performance concrete and its mitigation using superabsorbent polymer based internal curing method, Cem. Concr. Compos., 89 (2018) 130-138. https://doi.org/10.1016/j.cemconcomp.2018.03.003

[20] M. Reda, N. Shrive, and J. Gillott, Microstructural investigation of innovative UHPC, Cem. Concr. Res., 29 (1999) 323-329. https://doi.org/10.1016/S0008-8846(98)00225-7

[21] D. Wang, C. Shi, Z. Wu, J. Xiao, Z. Huang, and Z. Fang, A review on ultra high performance concrete: Part II. Hydration, microstructure and properties, Constr. Build. Mater., 96 (2015) 368-377. https://doi.org/10.1016/j.conbuildmat.2015.08.095

[22] N. P. C. Association, Ultra High Performance Concrete (UHPC) Guide to Manufacturing Architectural Precast UHPC Elements, National Precast Concrete Association: Carmel, CA, USA, 2013.

[23] A. I. Khuri and S. Mukhopadhyay, Response surface methodology, Wiley Interdiscip. Rev. Comput. Stat., 2 (2010) 128-149. https://doi.org/10.1002/wics.73

[24] E. Ghafari, H. Costa, and E. Júlio, RSM-based model to predict the performance of self-compacting UHPC reinforced with hybrid steel micro-fibers, Constr. Build. Mater., 66 (2014) 375-383. https://doi.org/10.1016/j.conbuildmat.2014.05.064

[25] ASTM, Standard specification for Portland cement (ASTM-C150/C150M), West Conshohocken, Pennsylvania: ASTM International., A. S. f. T. a. M. International, (2015a).

[26] ASTM, Standard specification for silica fume used in cementitious mixtures (ASTM C1240-15), West Conshohocken, Pennsylvania: ASTM International., A. S. f. T. a. M. International, (2015b).

[27] ASTM, Standard test method for flow of hydraulic cement mortar (ASTM C1437), West Conshohocken, Pennsylvania: ASTM International., A. S. f. T. a. M. International, (2020a).

[28] ASTM, Standard test method for compressive strength of hydraulic cement mortars using 2-in. or 50-mm cube specimens (ASTM C109/C109M-11b). West Conshohocken, Pennsylvania: ASTM International., A. S. f. T. a. M. International, (2010a).

[29] A. M. Rashad, An exploratory study on alkali-activated slag blended with quartz powder under the effect of thermal cyclic loads and thermal shock cycles, Constr. Build. Mater., 70 (2014) 165-174. https://doi.org/10.1016/j.conbuildmat.2014.06.097

[30] A. M. Rashad and A. S. Ouda, An investigation on alkali-activated fly ash pastes modified with quartz powder subjected to elevated temperatures, Constr. Build. Mater., 122 (2016) 417-425.https://doi.org/10.1016/j.conbuildmat.2016.06.068

[31] J. A.-G. N. T.-C. D. C. Jaramillo-Murcia and E. García-Castaño, Properties Analysis of Ultra-High-Performance Concrete with Recycled Glass and Limestone Powders, ACI Matet. J., 119 (2022) 153-164. https://doi.org/10.14359/51736006

[32] Z. Wu, C. Shi, and W. He, Comparative study on flexural properties of ultra-high performance concrete with supplementary cementitious materials under different curing regimes, Constr. Build. Mater., 136 (2017) 307-313. https://doi.org/10.1016/j.conbuildmat.2017.01.052

[33] R. Yu, P. Spiesz, and H. Brouwers, Mix design and properties assessment of ultra-high performance fibre reinforced concrete (UHPFRC), Cem. Concr. Res., 56 (2014) 29-39. https://doi.org/10.1016/j.cemconres.2013.11.002